Myoglobin O_2 Desaturation during Exercise

Evidence of Limited O_2 Transport

Russell S. Richardson,* Elizabeth A. Noyszewski,‡ Keith F. Kendrick,‡ John S. Leigh,‡ and Peter D. Wagner*

**Department of Medicine, University of California, La Jolla, California 92093-0623; and ‡Department of Radiology, University of Pennsylvania, Philadelphia, Pennsylvania 19104-6021*

Abstract

The assumption that cellular oxygen pressure (P_{O_2}) is close to zero in maximally exercising muscle is essential for the hypothesis that O_2 transport between blood and mitochondria has a finite conductance that determines maximum O_2 consumption. The unique combination of isolated human quadriceps exercise, direct measures of arterial, femoral venous P_{O_2}, and ^1H nuclear magnetic resonance spectroscopy to detect myoglobin desaturation enabled this assumption to be tested in six trained men while breathing room air (normoxic, N) and 12% O_2 (hypoxic, H). Within 20 s of exercise onset partial myoglobin desaturation was evident even at 50% of maximum O_2 consumption, was significantly greater in H than N, and was then constant at an average of 51±3% (N) and 60±3% (H) throughout the incremental exercise protocol to maximum work rate. Assuming a myoglobin P_{O_2} where 50% of myoglobin binding sites are bound with O_2 of 3.2 mmHg, myoglobin-associated P_{O_2} averaged 3.1±.3 (N) and 2.1±.2 mmHg (H). At maximal exercise, measurements of arterial P_{O_2} (115±4 [N] and 46±1 mmHg [H]) and femoral venous P_{O_2} (22±1.6 [N] and 17±1.3 mmHg [H]) resulted in calculated mean capillary P_{O_2} values of 38±2 (N) and 30±2 mmHg (H). Thus, for the first time, large differences in P_{O_2} between blood and intracellular tissue have been demonstrated in intact normal human muscle and are found over a wide range of exercise intensities. These data are consistent with an O_2 diffusion limitation across the 1–5-μm path-length from red cell to the sarcolemma that plays a role in determining maximal muscle O_2 uptake in normal humans. (*J. Clin. Invest.* 1995. 96:1916–1926.) Key words: quadriceps • blood flow • diffusional conductance • myoglobin • magnetic resonance spectroscopy

Introduction

The complete oxygen cascade from the air to mammalian tissue has been challenging to study in vivo. The final two levels in this cascade, capillary oxygen pressure (P_{O_2})[1] and intracellular P_{O_2}, are probably of most interest and have remained the most elusive. Recently, however, the ability to detect myoglobin desaturation using proton magnetic resonance spectroscopy (MRS) has made it possible to estimate intracellular P_{O_2} (1). Proton MRS, unlike most previous techniques that address tissue oxygenation, is noninvasive, is without deleterious effects, and therefore is suitable for in vivo human studies (2). Effluent venous P_{O_2} reflects mean end-capillary P_{O_2} in an isolated muscle (3), thus if both arterial and venous P_{O_2} are measured, a value for mean capillary P_{O_2} can be computed, and from this a diffusional conductance (DO_2) can be determined assuming mitochondrial $P_{O_2} = 0$ and residual venous O_2 reflects only diffusion limitation of O_2 transport (4). The functional isolation of the quadriceps muscle group has previously been used to study exercising muscle in humans (5) and allows the measurement of effluent (femoral) venous P_{O_2} and the calculation of mean capillary P_{O_2} (6).

By combining the isolated quadriceps muscle model (5) and proton MRS technology to detect myoglobin saturation (1), it is possible to study the complete series of oxygen gradients from ambient air to human muscle in vivo during dynamic exercise. The present study uses this unique combination of methodologies to test the hypothesis that during exercise intracellular P_{O_2} is much lower than capillary P_{O_2}, which would confirm the importance of the blood to mitochondrial O_2 conductance pathway in determining maximum oxygen uptake ($\dot{V}O_{2max}$). Specifically, MRS techniques were used to detect simultaneously proton and phosphorous levels in the quadriceps muscle group during dynamic incremental knee-extensor exercise breathing both 21 and 12% O_2. Proton MRS allowed the determination of myoglobin saturation, and ^{31}P data were collected to characterize the muscles metabolic activity during this mode of incremental exercise and to act as an independent measure of metabolic demand. 2 wk before these MRS measurements, using femoral vein and radial artery catheterization, arterial P_{O_2}, femoral venous P_{O_2}, and muscle blood flow were directly measured in the same subjects during identical work profiles to relate intravascular P_{O_2} to intramuscular values.

Methods

Subjects. All six healthy, nonsmoking male subjects were competitive athletes who regularly bicycled 200–400 miles per wk. Health histories

Address correspondence to Russell S. Richardson, Department of Medicine 0623A, 9500 Gilman Drive, University of California, La Jolla, CA 92093-0623. Phone: 619-534-9841; FAX: 619-534-4812.

Received for publication 27 December 1994 and accepted in revised form 1 June 1995.

J. Clin. Invest.

0021-9738/95/10/1916/11 $2.00
Volume 96, October 1995, 1916–1926

1. *Abbreviations used in this paper:* CaO_2, arterial oxygen concentration; CvO_2, venous oxygen concentration; DO_2, oxygen diffusional conductance; FID, free-induction decay; H, hypoxic; Hb, hemoglobin; MRS, magnetic resonance spectroscopy; Mb, myoglobin; N, normoxic; P_{50}, oxygen pressure where 50% of myoglobin binding sites are bound with oxygen; P_{CAPo2}, capillary P_{O_2}; P_{MITOo2}, mitochondrial P_{O_2}; P_{MbO2}, myoglobin P_{O_2}; P_{O_2}, oxygen pressure; PCr, creatine phosphate; Pi, inorganic phosphate; $\dot{Q}$, blood flow; $\dot{V}O_2$, oxygen uptake; $\dot{V}O_{2max}$, maximum $\dot{V}O_2$; WR, work rate; WR_{MAX}, maximum WR.

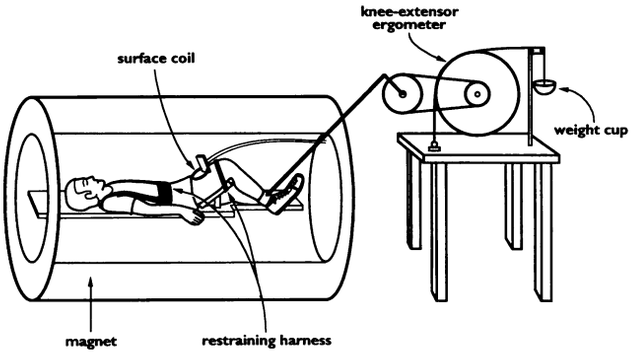

Figure 1. The arrangement of the nonmetallic knee-extensor and the subject, allowing dynamic exercise in the bore of the 2 Tesla magnet.

and a physical examination were completed on each subject. All subjects were without history of cardiopulmonary disease and upon physical examination were within normal limits. As this research was performed in two laboratories, informed consent was obtained according to both the University of California San Diego and the University of Pennsylvania Institutional Review Board for Human Subjects Research Committees.

Overview of experimental protocol. This research studied one group of subjects in two locations; subjects were initially studied in San Diego, CA, and were then transported to Philadelpnia, PA and studied again. In San Diego, to facilitate the learning of the unfamiliar knee-extensor exercise, all subjects performed five to six training bouts on the knee-extensor apparatus before data collection. The final two practices included a graded maximal knee-extensor exercise test and a protocol that simulated the planned experiment. On the final San Diego test day, after the catheterization of the femoral vein and radial artery (explained in detail below), two bouts of exercise were performed: left leg quadriceps exercise breathing room air (21% O_2) and left leg quadriceps exercise breathing 12% O_2. The sequence of these exercise bouts across subjects was reversed in three subjects to avoid ordering artifacts. For each bout, exercise work rate (WR) was increased from 25 to 50 to 75 and then to 90 and 100% of normoxic (N) maximum WR (WR_{MAX}) with data obtained at each level. After a 2–3-min period at each work rate, sufficient to attain constant pulmonary oxygen uptake ($\dot{V}O_2$) (7), the sequence of events at each work rate was as follows: (a) 3-ml blood samples were taken, and (b) femoral vein blood flow was measured. Duplicate measurements of all variables were then taken without delay, to keep total exercise time to a minimum. Each incremental exercise bout was completed in 10–16 min.

Within 2 wk of completing the final San Diego study, subjects traveled by airplane to Philadelphia. In Philadelphia, the 7-cm surface coil was strapped to the anterior portion of the quadriceps. Initial resting measurements (2 min) were made and then ischemic measurements (10 min) were made through the inflation of a thigh cuff to 270 mmHg (proximal to the surface coil) with the subject positioned in the bore of the magnet, as for exercise (Fig. 1). After the removal of the thigh cuff and a 30-min recovery period, subjects reproduced both the normoxic and hypoxic (H) exercise protocols performed in San Diego, but without vascular catheterization. Exercise loads, WRs, and times were set to exactly reproduce the exercise profile achieved in San Diego. Throughout rest and exercise both proton MRS and ^{31}P MRS data were collected with 20-s resolution.

Specifics of exercise study with blood flow ($\dot{Q}$) and blood gas measurements in San Diego. Two catheters (radial artery and left femoral vein) and a thermocouple (left femoral vein) were emplaced using sterile technique as previously reported (8, 9). A 20-gauge, 3.2-cm long arterial catheter was inserted percutaneously under local anesthesia (1% lidocaine) in the radial artery of the nondominant hand for arterial blood sampling. Subsequently, a catheter 1.25 mm in external diameter (DSA 400L; Cook, Bloomington, IN) was introduced percutaneously into the left femoral vein 2 cm below the inguinal ligament and advanced 7 cm distally. This catheter has an open end and also 10 pinhole side ports in the distal 2.5 cm oriented in all directions around the catheter. This ensures that during injection of cold saline for thermodilution flow measurement, thin streams are ejected at all orientations into the vein facilitating mixing across the vein lumen. This mixing was confirmed during in vitro model testing of the technique, with colored dye injection and video analysis. The second catheter consisted of a thin (0.64-mm diameter) polyethylene-coated thermocouple (IT-18; Physitemp Instruments, Clifton, NJ) that was advanced from approximately the same location proximally 10 cm into the left femoral vein toward the heart. Each catheter was attached to the skin using adhesive tape and positioned so as to minimize the risk of movement or creasing. During exercise, iced saline was infused through the femoral venous catheter at flow rates sufficient to decrease blood temperature at the thermocouple by $\approx$ 1°C. Infusions were continued for 15–20 s until femoral vein temperature had stabilized at its new lower value. Saline injection rate was measured by weight change in a reservoir bag suspended from a force transducer which was calibrated before and after each experiment. The calculation of blood flow was performed on thermal balance principles as detailed by Andersen and Saltin (10). This method of measuring blood flow has been used on several occasions in research from this and other laboratories (8–13). In each of these experiments and in this study, the ultimate criterion of validity (which currently in intact humans can only be whether the measurements of blood flow and arterial–venous differences yield proper values for oxygen uptake) (8) was achieved based on the slopes of the $\dot{V}O_2$–WR relationship. In a previous paper from this group (9), a detailed consideration of putative sources of error and steps which reduce their influence was published. Precautions noted therein were carefully followed throughout this study.

The samples of arterial and venous blood were used to measure P_{O_2}, CO_2 pressure, pH, O_2 saturation, and hemoglobin. All measurements were made on a blood gas analyzer (IL 1306; Instrumentation Laboratories, Inc., Lexington, MA) and a CO-oximeter (IL 282; Instrumentation Laboratories). Between each sample, electrodes were calibrated and demonstrated acceptable reproducibility (SD of repeated determinations: P_{O_2} and CO_2 pressure, 1.5 mmHg; pH, 0.003). Blood lactate concentration was determined using a blood lactate analyzer (1500; Yellow Springs Instrument Co., Yellow Springs, OH). Blood O_2 concentration was calculated as 1.39 × [hemoglobin (Hb)] × measured O_2 saturation + 0.003 × measured P_{O_2}. Arterial–venous [O_2] difference was calculated from the difference in radial artery and femoral venous oxygen concentration. This difference was then divided by arterial concentration to give O_2 extraction. Leg $\dot{V}O_2$ was calculated as the product of arterial–venous O_2 concentration difference and blood flow.

Throughout testing in San Diego, subjects breathed through a low resistance two-way breathing valve (2700; Hans-Rudolph Inc., Kansas City, MO). Expired gas passed into a 7.2-liter heated, low resistance mixing chamber and was continuously sampled from a multiport manifold by an MGA 1100 mass spectrometer (Perkin-Elmer Corp., Norwalk, CT) (inflow rate, 20 ml · min^{-1}). Expired gas flow was measured by a pneumotachograph (Fleisch No. 3; Hans-Rudolph Inc.). Electrical signals from the mass spectrometer and pneumotachograph were logged at 100 Hz by use of a 12-bit analogue-to-digital converter for a determination of ventilation (body temperature, pressure, saturated with water vapor) and gas exchange ($\dot{V}O_2$ and CO_2 uptake) (standard temperature, pressure, dry) by a commercially available software package (Consentius Technologies, Salt Lake, UT). $\dot{V}O_2$ and respiratory exchange ratio were displayed graphically, averaged over 30 s, for real-time monitoring of gas exchange. Repeated calibrations with this system established both volumetric and gas exchange accuracy to within 2%, confirmed by Douglas bag collections of expired gas and Tissot spirometry.

Specifics of exercise study with MRS measurements in Philadelphia. Within 2 wk of the San Diego exercise study with leg $\dot{Q}$ and blood gas measurements, subjects were transported to Philadelphia where the exercise protocol was reproduced in a 2.0 Tesla imaging magnet with custom-built spectrometer (Oxford Instruments, Cambridge, UK) (Fig. 1). A 7-cm diameter surface coil double-tuned to proton (85.45 MHz) and phosphorus (34.59 MHz) was placed over the rectus femoris portion

of the quadriceps group, ~ 20–25 cm proximal to the knee (14). Spectra were collected from the muscle region beneath the surface coil. This region, as determined from scout images (data not shown) and previous calculations of surface coil sensitivity is largely confined to a semispherical volume defined by the coil circumference and penetrating to a depth equal to the radius of the coil. For these studies, this "sensitive region" was 100 cm^3, which isolated signal detection predominantly from the region of the rectus femoris.

Details of the theory behind oxygen-sensitive myoglobin (Mb) signals have been published previously (15). The heme iron exhibits oxygen-dependent spin states that in turn influence nearby protons. The N-δ proton on proximal histidine F8, one of the ligands coordinated to the iron, is particularly sensitive to these changes. When oxygen is bound to the active site, the resonance of this proton is hidden beneath the dominant water signal. However, when myoglobin becomes deoxygenated, changes in the iron spin-state shift this peak to a temperature-dependent position that is clearly distinct from all other resonances. At physiological temperature, this peak resonates ~ 73 ppm downfield from the water resonance. This oxygen-dependent signal can be calibrated to obtain values for myoglobin desaturation; these values can be converted to intracellular oxygen tensions using oxygen-binding curves for myoglobin.

After placing the subject in the magnet, the coil was centered in the homogeneous portion of the magnetic field by aligning the water resonance in the center of applied x, y, and z gradient fields. The main magnetic field was then shimmed until the linewidth of the water resonance at half-height decreased to < 20 Hz (17.8±0.5 Hz, mean±SD). After this, the nominal 90° hard pulses were calibrated at both frequencies. They averaged 0.153±0.004 ms for proton and 0.143±0.005 ms for phosphorus. This indicated that the B1 fields for the two frequencies differed by < 7%, which indicated that the proton and phosphorus signals arose from matching sample volumes.

Proton and phosphorus spectra were obtained using a modified super-WEFT water suppression sequence (Noyszewski, E., R. Reddy, Z. Wang, and J. S. Leigh, manuscript in preparation). For proton data, water and fat resonances were inverted using a 12-ms hyperbolic secant pulse with inversion bandwidth = 2 kHz. 65 ms later, the remaining spins were excited with a 0.5-ms gaussian pulse centered 6,650 Hz downfield from the water resonance frequency. This gaussian pulse had previously been calibrated on the water resonance to achieve the same signal intensity as the nominal 90° proton hard pulse. Proton free-induction decays (FIDs) were then sampled over a spectral bandwidth = 20 kHz using 512 points and dwell time = 50 μs. Total repetition time = 130 ms for this sequence. This sequence was paused every 4 s to collect phosphorus data in an interleaved manner. After excitation with a nominal 90° hard pulse (0.143±0.005 ms), phosphorus FIDs were sampled over a spectral bandwidth = 2 kHz using 512 points and dwell time = 500 μs. 24 proton FIDs were collected for every phosphorus FID. For each 20-s time point this corresponded to 120 proton signal averages and 5 phosphorus signal averages.

During the entire study and particularly during the exercise, precautions were taken to minimize unnecessary movement that could alter signal intensity. The subject was securely fastened at the shoulders, waist, and knee before data collection. Subjects were also instructed to minimize any movement beyond the intended exercise. In addition, to determine if motion was a problem, the water resonance was checked periodically for possible changes in position or linewidth. The resonance did not move by > 0.1 ppm or increase in width > 2 Hz for any of the subjects, indicating that motion did not degrade the signal during the study.

After acquisition, proton and phosphorus FIDs were apodized with exponentially weighted functions: for proton this corresponded to 100 Hz of line broadening in the frequency domain while for phosphorus the line broadening was 5 Hz. The FIDs were then Fourier transformed and manually phased to generate the frequency spectra. For the phosphorus spectra, areas were determined through integration of the peaks arising from inorganic phosphate (Pi), creatine phosphate (PCr), and b-ATP resonances. Conversion to concentration units was then accomplished by normalizing signal areas to the ATP value at rest, assuming resting ATP = 8.2 mM (16). Pi/PCr values were also computed as an index of the bioenergetic state of the muscle tissue (17). Intracellular pH was calculated from the parts per million difference between Pi and PCr peaks, using the formula cited by Taylor et al. (18).

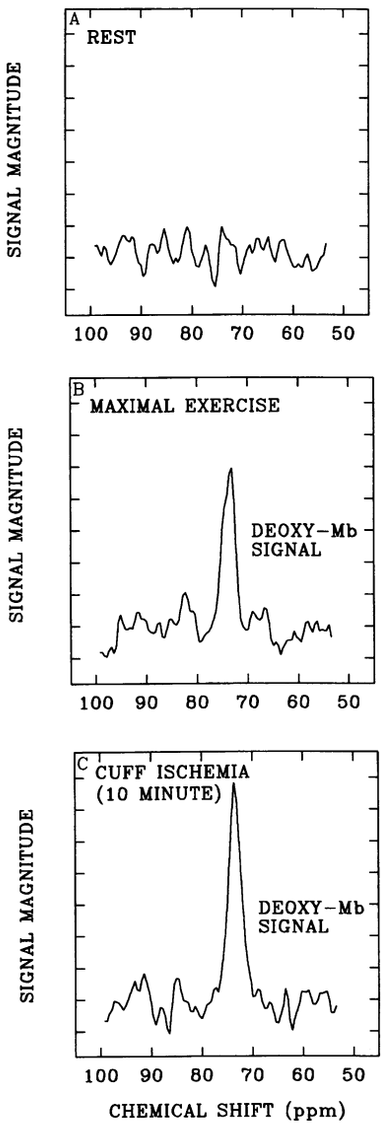

Figure 2. Three representative individual deoxy-Mb spectra collected at rest (*A*), during maximal exercise (*B*), and at 10 min of suprasystolic cuff occlusion (*C*).

For the proton spectra, areas were obtained under the peak resonating ~ 73 ppm down-field from the residual water signal (Fig. 2). Before analysis, the outer 128 points on either side of the spectrum were removed. The remaining portion was baseline corrected by fitting the spectrum to a fifth-order polynomial in the frequency domain, which was then subtracted from the spectrum. To ensure that deoxy-Mb resonances were not altered, the spectrum in the region 65–80 ppm downfield from the water resonance was removed before the baseline routine. After baseline correction, spectra were manually phased, and areas were obtained through integration of the peak arising 73 ppm from the water resonance. The peak position remained relatively constant throughout the protocol, averaging 73.2±0.1 ppm during the last 2 min of cuffing, 73±0.1 ppm during the normoxic exercise, and 72.8±0.1 ppm during the hypoxic bout. No other peaks were visible within 10 ppm of the deoxy-Mb resonance at any time. Although deoxy-Hb in solution gives rise to signals in the region of the deoxy-Mb peak (19), it has previously been shown that the visibility of deoxy-Hb in vivo is greatly reduced compared to that of deoxy-Mb (20).

Fraction deoxy-Mb was determined by normalizing signal areas to the average signal obtained during the 9th and 10th min of a cuff ischemia at suprasystolic pressure (265 mmHg). At rest, intramuscular oxygen depletes within 6–8 min of occlusion (21). Therefore the signals obtained during the last 2 min of the cuff represent complete deoxygenation of myoglobin and may be used to estimate total Mb content within the muscle. Conversion to P_{O_2} values were then calculated from the well-known oxygen-binding curve for myoglobin:

$$P_{O_2} = [(1 - f)/f] \cdot P_{50} \quad (1)$$

where 1 − f is the fraction of myoglobin that is oxygenated, f is the fraction of myoglobin that is not oxygenated, and P_{50} is the oxygen pressure where 50% of the myoglobin binding sites are bound with oxygen. The temperature-dependent myoglobin P_{50} of 3.2 mmHg was used (22), based on an approximate muscle temperature of 39°C (23). However, as we report both saturation and myoglobin associated P_{O_2}, the latter can be recalculated at any P_{50}.

Exercise model. The knee-extensor ergometer was designed and constructed in the Johnson Foundation (Philadelphia, PA) for the left (instrumented) leg to replicate the device reported in previous research (5, 8, 10, 13) (Fig. 1). This ergometer was constructed from nonmetallic materials to allow its use in both the human physiology lab in San Diego and the MRS facility in Philadelphia. The subject lay supine on a padded bed with the knee-extensor ergometer placed in front of him. The resistance to knee-extension was provided via a fiberglass bar attached to the crank of the ergometer and to a specially designed shin brace worn by the subject (Fig. 1). This ergometer was a prototype, and as such WR could not be measured in conventional units of work, but WR was prescribed and measured as a percentage of the maximum resistance (weight [g], resisting the fly-wheel turning, Fig. 1) at the end of the preliminary graded maximal test. 60 dynamic contractions of the knee-extensor muscles per min were performed. Contractions of the quadriceps femoris muscle caused the lower part of the leg to extend from ~ 90–170° flexion. Throughout the exercise the thigh remained immobile. This stability was enhanced by the 45° angle of the exercising leg and the harness worn by each subject (Fig. 1). The momentum of the flywheel returned the relaxed leg to the start position. This passive movement of the leg after contraction, anecdotal reports from subjects, and force tracings from a force transducer placed between the ergometer and the subject during this exercise (8) support the conclusion that active contraction was limited to the quadriceps muscles. The subjects were constrained in the bed by a safety belt which anchored the hips and shoulders (Fig. 1).

Mean capillary P_{O_2} and muscle DO_2. Using the measured intracellular P_{O_2} values, mean capillary P_{O_2} was calculated as described previously (4). Because these calculations used the measured myoglobin-associated P_{O_2}, they were no longer burdened by the assumption of a low intracellular P_{O_2} at WR_{MAX} (4). As a result, DO_2 calculations were performed for each WR using the corresponding intracellular P_{O_2} measurement and not just at 100% of WR_{MAX}, as in previous studies. A numerical integration procedure is used to determine that value of DO_2, assumed constant along the capillary, that produces the measured femoral venous P_{O_2}, given the measured arterial P_{O_2}. Additional explicit assumptions of this calculation are: the only explanation of O_2 remaining in the femoral venous blood is diffusion limitation of O_2 efflux from the muscle microcirculation. Perfusion/$\dot{V}O_2$ heterogeneity, and perfusional or diffusional shunt are considered negligible. To the extent that these phenomena contribute O_2 to femoral venous blood, the parameter DO_2 is a conductance coefficient that expresses the diffusional conductance that would be required to achieve the measured $\dot{V}O_2$, assuming only diffusion limitation. This assumption cannot be avoided currently for the lack of specific means for detecting perfusion/$\dot{V}O_2$ heterogeneity and shunt. Mean capillary P_{O_2} is the average of all P_{O_2} values computed at equal time intervals along the capillary from the arterial to the venous end. While mean capillary P_{O_2} is useful for graphical purposes (see Results), our conclusions come from statistical comparisons of DO_2 among the two experimental conditions.

Quadriceps femoris muscle mass. As suggested by Andersen and Saltin and others (8, 10, 24), thigh length, circumference, and skinfold measurements were used to determine thigh volume. This permitted an estimate of quadriceps muscle mass. It should be recognized that this calculation of muscle mass and the consequent normalizing of $\dot{Q}$ and $\dot{V}O_2$ assume that this is the only muscle mass involved in the knee-extensor exercise.

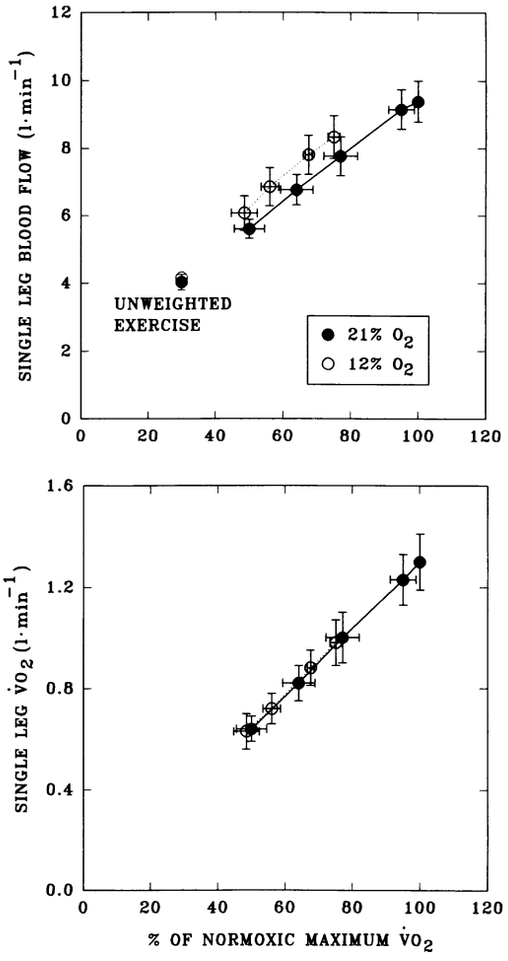

Figure 3. Single leg blood flow (*A*) and leg $\dot{V}O_2$ (*B*) in relation to the percentage of maximum normoxic work rate in both normoxia and hypoxia.

Statistical analyses. Least-squares regression, repeated measures ANOVA (Tukey post hoc), and Student's *t* test analyses were computed using a commercially available software package (PC+; SPSS Inc., Chicago, IL). Variables were considered significantly different when $P \leq 0.05$. Data are presented as the mean±SE throughout the manuscript.

Results

Subject characteristics and screening tests. The physical characteristics of the subjects were as follows (average±SE): age, 23.3±1.7 yr; height 181.2±1.7 cm; and weight 73.8±2.4 kg. As a part of this screening process, subjects performed a conventional incremental cycle ergometry test (100 W initial WR increased by 25 $W \cdot min^{-1}$ until fatigue), and their $\dot{V}O_{2max}$ averaged 4.4±0.1 liters $\cdot min^{-1}$ or 60.0±1.7 $ml \cdot kg^{-1} \cdot min^{-1}$ in this test.

Leg blood flow, leg $\dot{V}O_2$, and WR. During both normoxic and hypoxic exercise, the instrumented left leg demonstrated a

Table I. Major Physiological Variables Measured During Incremental Knee-extensor Exercise

Measured variable		Exercise level 1	Exercise level 2	Exercise level 3	Exercise level 4	Exercise level 5
Percentage of normoxic leg $\dot{V}O_{2max}$	N	50.0%±4.5	64.0%±4.8	77.0%±5.0	95.3%±3.8	100%±0
	H	48.5%±3.8	56.6%±2.6	67.5%±1.0	75.1%±1.8	—
CaO_2 (ml · 100 ml^{-1})	N	18.1±0.2	18.3±0.1	18.5±0.2	18.7±0.2	18.7±0.5*
	H	14.9±0.4‡	14.8±0.4‡	15.2±0.2‡	15.2±0.5‡	—
CvO_2 (ml · 100 ml^{-1})	N	6.7±0.9	6.1±0.8	5.7±0.8	4.9±0.7	4.7±0.7*
	H	4.5±0.6‡	4.1±0.5‡	3.8±0.5‡	3.4±0.5‡	—
Leg PvO_2 (mmHg)	N	26.3±1.3	25.1±1.5	24.4±1.5	22.6±1.4	22.1±1.6*
	H	20.3±0.9‡	19.3±1.1‡	18.6±1.4‡	17.4±1.3‡	—
Mean capillary PO_2 (mmHg)	N	42.0±1.5	42.4±1.6	40.1±1.7	38.4±1.5	37.5±1.6*
	H	30.8±0.9‡	30.4±1.2‡	30.2±1.9‡	29.7±1.5‡	—
Diffusional conductance (ml $O_2 \cdot min^{-1} \cdot mmhg^{-1}$)	N	15.7±0.2	21.0±0.3	24.9±0.4	33.7±0.3	35.3±0.3
	H	20.2±0.4‡	24.6±0.3‡	30.0±0.3‡	36.3±0.2‡	—
Deoxy-Mb signal (percentage of maximum cuff signal)	N	48±5	56±4	50±5	50±4	51±3*
	H	58±5‡	63±3‡	63±2‡	58±1‡	—
Mb-associated PO_2 (mmHg)	N	3.5±0.4	2.5±0.2	3.2±0.4	3.2±0.4	3.1±0.3*
	H	2.3±0.3‡	1.9±0.1‡	1.9±0.1‡	2.3±0.1‡	—
Leg $\dot{Q}$ (liters · min^{-1})	N	5.6±0.3	6.8±0.5	7.8±0.6	9.2±0.6	9.4±0.6*
	H	6.1±0.5	6.9±0.6	7.8±0.6	8.3±0.6	—
Leg O_2 delivery (liters · min^{-1})	N	1.0±0.1	1.2±0.1	1.4±0.1	1.7±0.1	1.7±0.1*
	H	0.9±0.1‡	1.0±0.1‡	1.2±0.1‡	1.3±0.1‡	—
Leg $\dot{V}O_2$ (liters · min^{-1})	N	0.64±0.05	0.82±0.07	1.00±0.10	1.23±0.10	1.3±0.1*
	H	0.63±0.07	0.72±0.06	0.88±0.07	0.98±0.09‡	—
Leg O_2 extraction (%)	N	62.9±4.7	66.6±4.3	69.3±4.1	73.6±3.5	74.8±3.4
	H	69.5±4.4‡	72.1±3.4‡	75.1±4.0‡	77.6±3.3‡	—
Arterial pH	N	7.372±0.01	7.369±0.01	7.363±0.01	7.370±0.02	7.374±0.02
	H	7.420±0.01	7.403±0.01	7.404±0.01	7.404±0.01	—
Venous pH	N	7.293±0.01	7.263±0.01	7.220±0.02	7.206±0.02	7.209±0.02
	H	7.322±0.02	7.279±0.01	7.244±0.01	7.229±0.02	—
Arterial lactate (mM)	N	1.4±0.1	2.0±0.1	2.6±0.2	3.7±0.3	4.3±0.3
	H	1.5±0.1‡	2.5±0.1‡	3.8±0.1‡	4.8±0.2‡	—
Pulmonary $\dot{V}O_2$ (liters · min^{-1})	N	0.94±0.04	1.12±0.06	1.35±0.09	1.76±0.13	2.11±0.10
	H	0.97±0.04	1.15±0.05	1.63±0.11	2.04±0.08	—
Respiratory exchange ratio	N	0.8±0.07	0.92±0.06	1.06±0.03	1.11±0.04	1.12±0.03
	H	0.94±0.01	0.96±0.02	0.99±0.03	0.99±0.02	—
Heart rate (beats · min^{-1})	N	111.0±3.0	123.0±4.0	137.0±6.0	153.0±5.0	165.0±4.0
	H	118.0±1.4	130.0±2.0	150.0±4.0	158.0±4.0	—

Mean (±SE) percentage of normoxic leg $\dot{V}O_2$; arterial (CaO_2) and femoral venous (CvO_2) O_2 content; leg venous partial pressure of O_2 (PvO_2); mean capillary partial pressure of O_2 (PO_2); diffusional conductance of O_2; deoxy-myoglobin (deoxy-Mb) saturation; myoglobin (Mb) associated partial pressure of oxygen (PO_2); leg blood flow ($\dot{Q}$); O_2 delivery; leg $\dot{V}O_2$; O_2 extraction; arterial pH; venous pH; arterial lactate concentration; pulmonary $\dot{V}O_2$; respiratory exchange ratio, and heart rate during knee-extensor exercise in normoxic (N) and hypoxic (H) conditions. * Significantly different from normoxic values at maximal exercise ($P \leq 0.05$). ‡ Significantly different relationship from normoxic values across all exercise intensities ($P \leq 0.05$).

linear rise in both leg $\dot{Q}$ and leg $\dot{V}O_2$ as WR increased towards WR_{MAX} (Fig. 3, Table I). Leg $\dot{Q}$ and leg $\dot{V}O_2$ rose to high mass-specific levels corresponding quantitatively with previous reports (6, 8, 25) (Fig. 3, Table I). At submaximal work rates there was no significant difference in the relationship between leg $\dot{Q}$ and WR or leg $\dot{V}O_2$ and WR between the two conditions (Fig. 3, Table I). However, maximal leg $\dot{Q}$, leg $\dot{V}O_{2max}$, and WR_{MAX} were all significantly reduced in hypoxia ($P \leq 0.05$) (Fig. 3, Table I). It is important to note that this prototype nonmetallic ergometer required an appreciable amount of work during "unweighted" exercise (Fig. 3). As this internal work of the ergometer was not measurable, the metabolic cost of producing each WR (increased by the addition of weight to a belt around the flywheel) was related in a different fashion to conventional cycle ergometry (i.e., 25% of WR_{MAX} = 50% of leg $\dot{V}O_{2max}$, 50% of WR_{MAX} = 65% of leg $\dot{V}O_{2max}$, etc., Table I). To avoid incorrect implications of the present results, in relation to a percentage of WR_{MAX} and other exercise ergometers, all data have been expressed in relation to the percentage of normoxic single leg $\dot{V}O_{2max}$.

Intravascular Po_2 and muscle DO_2. In hypoxia at submaximal leg $\dot{V}O_{2max}$, arterial PO_2, venous PO_2, and calculated mean capillary PO_2 were also significantly lower than in normoxia ($P \leq 0.05$) (Table I, Fig. 4). At the reduced hypoxic leg $\dot{V}O_{2max}$

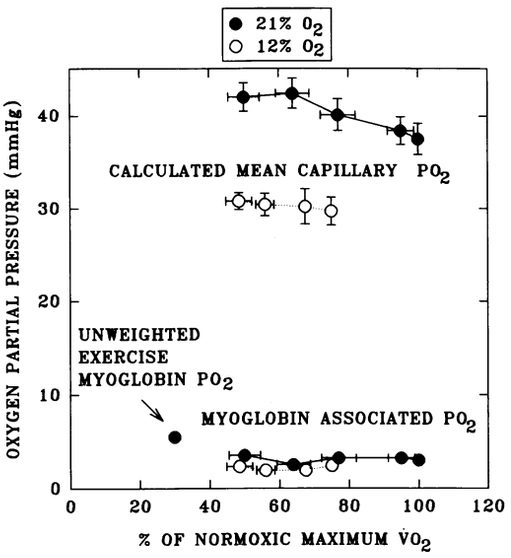

Figure 4. Calculated mean capillary P_{O_2} and cellular myoglobin-associated P_{O_2} in relation to the percentage of maximum normoxic $\dot{V}O_2$ in both normoxia and hypoxia. Note the large difference between the P_{O_2} available in the capillaries and the P_{O_2} at the cellular level, even at submaximal work rates.

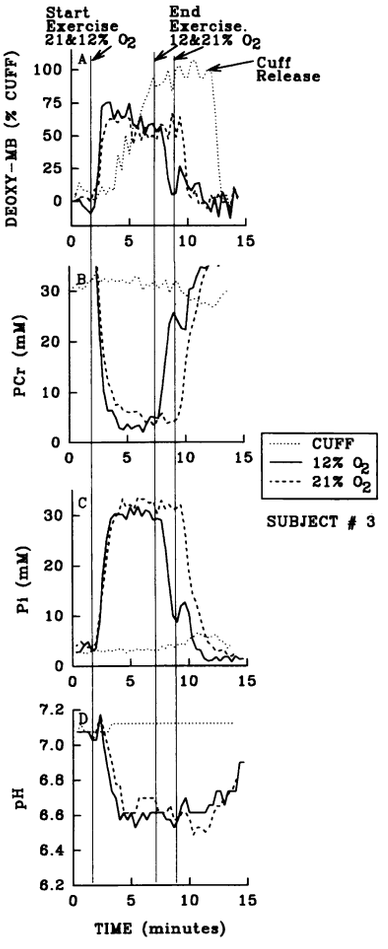

Figure 6. A representative individual set of magnetic resonance spectroscopy data collected during rest with a thigh cuff inflated to 270 mmHg proximal to the surface coil and then during continuous incremental knee-extensor exercise in normoxia and hypoxia. These data represent the measurement of myoglobin saturation (*A*), inorganic phosphate (*B*), phosphocreatine (*C*), and pH (*D*) with 20-s resolution.

both venous P_{O_2} and calculated mean capillary P_{O_2} were also significantly lower than at $\dot{V}O_{2max}$ in normoxia ($P \leq 0.05$) (Table I, Fig. 4). In both hypoxia and normoxia the calculated tissue DO_2 increased as the intensity of work increased (Fig. 5 *A*). At each submaximal WR, < 90%, the calculated DO_2 was elevated in hypoxia in comparison to normoxia ($P \leq 0.05$) (Table I, Fig. 5 *A*), but due to the greater continued rise in normoxic tissue DO_2 there was no significant difference in DO_2 between normoxia and hypoxia at WR_{MAX} (Table I, Fig. 5). This was the case no matter whether mean capillary or femoral venous P_{O_2} was used to illustrate muscle DO_2 (Fig. 5 *B*).

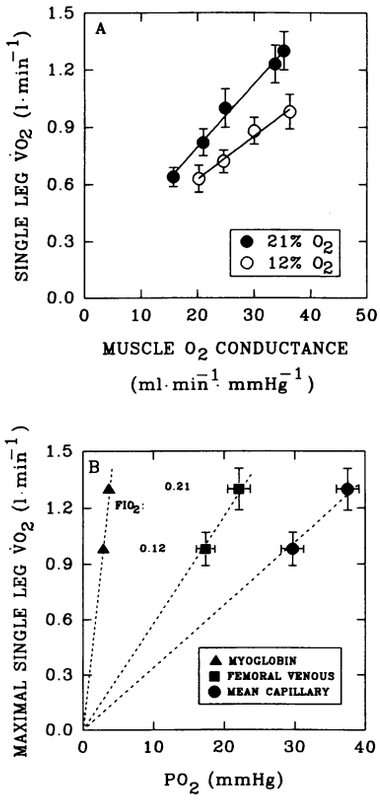

Figure 5. The relationship between $\dot{V}O_2$ and muscle O_2 conductance (*A*) and the relationship among $\dot{V}O_{2max}$ and myoglobin, femoral venous, and calculated mean capillary P_{O_2} in normoxa and hypoxia (*B*). Until the measurement of myoglobin-associated P_{O_2} was achieved in this study, this analysis of diffusivity was only possible at $\dot{V}O_{2max}$ where mitochondrial P_{O_2} was assumed very close to zero and so could be ignored. At these submaximal levels, diffusional conductance was greater in hypoxia (*A*), but as the maximal attainable work rate was approached myoglobin-associated P_{O_2}, calculated mean capillary, and femoral venous P_{O_2} in hypoxia and normoxia exhibit proportionality to the achieved leg $\dot{V}O_{2max}$ (*B*).

Intracellular P_{O_2}. Under resting conditions the proton resonances from myoglobin lay under the water peak, and the deoxymyoglobin signal was not evident (Fig. 2 *A*). After inflation of the thigh cuff, proximal to the surface coil, the deoxy-myoglobin signal increased for the initial 6 min and plateaued for the final 4 min as in previous research (1) (Figs. 2 *C* and 6 *A*). Based upon this plateau in the deoxy-Mb signal amplitude (Figs. 2 *C* and 6 *A*) and a previous MRS study of anoxic resting skeletal muscle (21), this signal averaged over minutes 9 and 10 of vascular occlusion was considered to be 100% of the deoxy-Mb signal. Before commencing the exercise protocol there was again no discernible deoxy-myoglobin signal. During unweighted knee-extensor exercise the deoxy-myoglobin signal rose to an average of 38% of the maximal deoxy-myoglobin signal (P_{MbO_2} = 5 Torr) (Figs. 4 and 7). In normoxia, as exercise progressed the deoxy-myoglobin signal increased rapidly (within 20 s to ≈ 50% of the maximum signal (P_{MbO_2} = 3.1 mmHg) and maintained this value until WR_{MAX} (Figs. 2 *B*, 4, 6, and 7). During hypoxic exercise the deoxy-myoglobin signal also increased rapidly to ≈ 60% of the maximum signal (P_{MbO_2} = 2.1 mmHg) and maintained this value through

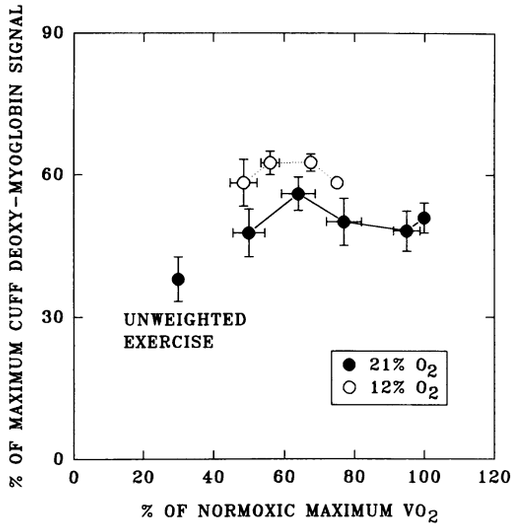

Figure 7. The percentage of maximum cuff deoxy-myoglobin signal in hypoxia and normoxia as a function of the percentage of maximum normoxic leg $\dot{V}O_2$ during knee-extensor exercise.

WR_{MAX} (Figs. 2 *B*, 4, 5, and 6). In both conditions, the cessation of exercise, after reaching WR_{MAX}, produced a rapid reduction in the deoxy-myoglobin signal and therefore a large increase in P_{MbO_2} within 20 s (Fig. 6 *A*).

O_2 delivery and O_2 extraction. In normoxic and hypoxic exercise, arterial O_2 content was independent of increasing work rate ($P \geq 0.05$) but was lower in hypoxia as expected (Table I). Femoral venous O_2 content decreased as work rate was increased ($P \leq 0.05$) (Table I). As the leg $\dot{Q}$ to WR relationship was similar in normoxia and hypoxia, muscle O_2 delivery to the leg was significantly reduced in hypoxia in comparison to normoxia ($P \leq 0.05$) (Table I). Throughout submaximal exercise, muscle O_2 extraction [$(CaO_2\text{-}CvO_2)/CaO_2$] was significantly higher in hypoxia than normoxia ($P \leq 0.05$) (Table I), where CaO_2 is arterial oxygen concentration and CvO_2 is venous oxygen concentration.

Muscle metabolism. Initial levels of PCr and Pi at rest were consistent with previous research (26) and were rapidly affected by the beginning of exercise. At the initial WR, which elicited $\approx$ 50% of leg $\dot{V}O_{2max}$, PCr fell and Pi rose to levels previously associated with this level of exercise intensity (26) (Table II, Fig. 6). The PCr/Pi index fell to a near nadir at $\approx$ 65% of leg $\dot{V}O_{2max}$, illustrating the high intensity of the muscular work during knee-extensor exercise. There were no significant differences in these variables between exercise in normoxia and hypoxia (Table II).

Intravascular and intracellular pH. Arterial pH was maintained at close to resting values in both normoxic and hypoxic conditions and was not significantly different in either condition during submaximal or maximal WRs. Venous pH fell with increasing exercise intensities in both conditions and was not different between hypoxia and normoxia (Table II). Intracellular pH also fell to low levels with increasing leg $\dot{V}O_2$ and was also not significantly different in hypoxia than in normoxia (Table II).

Quadriceps femoris weight. Estimated average quadriceps femoris weight was 2.5±0.14 kg. This allowed the calculation of mass specific $\dot{Q}$ and $\dot{V}O_2$ in normoxia and hypoxia which were 375±24 and 333.1±26 ml·min^{-1}·100 g^{-1} and 52.0±4.4 and 39.3±3.8 ml·min^{-1}·100 g^{-1}, respectively, at WR_{MAX}.

Discussion

The results of this study, in terms of leg $\dot{V}O_2$ and leg $\dot{Q}$, revealed high mass-specific values similar to previous studies in trained subjects exercising from submaximum to maximum levels with the quadriceps (6, 8) (Table I, Fig. 3). As in these previous studies, arterial P_{O_2} remained relatively constant in both hypoxia and normoxia as WR was increased and venous P_{O_2} fell progressively (6, 8) (Table I). From these data, mean capillary values were calculated to be 37±2 (N) and 30±2 mmHg (H) (Table I). Proton MRS measurements revealed a rapid desaturation of myoglobin, and thus myoglobin associated P_{O_2} fell quickly to an average of 3.1±.3 (N) and 2.1±.2 mmHg (H) which was then maintained through submaximal to maximal WRs (Table I).

These data represent the first experimental evidence of a steep O_2 gradient from blood to intracellular sites in human skeletal muscle in vivo. These independent numerical estimates

Table II. Indices of Muscle Metabolism During Incremental Knee-extensor Exercise

Measured variable		No exercise	Exercise level 1	Exercise level 2	Exercise level 3	Exercise level 4	Exercise level 5
Percentage of normoxic leg $\dot{V}O_{2max}$	N	Rest	50.0%±4.5	64.0%±4.8	77.0%±5.0	95.3%±3.8	100%±0.0
	H	Rest	48.5%±3.8	56.5%±2.6	67.5%±1.0	75.1%±1.8	—
PCr (mM)	N	38.2±2.5	13.0±1.9	6.4±1.1	3.4±0.5	3.1±0.3	3.0±0.3
	H	38.0±1.4	13.1±2.0	7.0±1.9	3.7±1.0	3.4±0.8	—
Pi (mM)	N	3.3±0.6	23.4±1.5	28.5±1.5	30.3±1.7	29.9±1.4	29.5±1.6
	H	2.8±0.5	21.6±1.9	25.1±1.3	27.0±0.9	26.5±0.8	—
PCr/Pi	N	11.5±4.1	0.6±1.3	0.2±0.7	0.1±0.4	0.1±0.2	0.1±0.2
	H	13.6±3.6	0.6±1.1	0.3±1.5	0.1±1.1	0.1±1.0	—
Intracellular pH	N	7.073±0.017	6.867±0.036	6.745±0.414	6.617±0.187	6.554±0.325	6.571±0.012
	H	7.119±0.044	6.691±0.076	6.535±0.094	6.464±0.084	6.394±0.147	—

Mean (±SE) percentage of maximum normoxic $\dot{V}O_{2max}$, intracellular creatine phosphate (PCr), intracellular inorganic phosphate (Pi), intracellular bioenergetic state (PCr/Pi), and intracellular pH.

reveal that O_2 pressure in the blood during exercise was 11–12-fold higher than in the cytoplasm at submaximal WRs (50% leg $\dot{V}O_{2max}$) and remained 8–10-fold higher even at WR_{MAX}. This equates to a P_{O_2} gradient from mean capillary blood to myoglobin of 39 (N) and 29 mmHg (H) at submaximal WRs, which fell slightly to 35 (N) and 27 mmHg (H) at WR_{MAX}. The determination of intravascular and intracellular P_{O_2} in this study allows an analysis of muscle diffusivity, less burdened by assumptions, throughout a range of exercise intensities in normoxia and hypoxia.

Muscle diffusional conductance. Muscle diffusivity can be described by Fick's law of diffusion:

$$\dot{V}O_2 = DO_2 (P_{CAPo2} - P_{MITOo2}) \quad (2)$$

Where DO_2 is muscle O_2 diffusional conductance and P_{CAPo2} is mean muscle capillary P_{O_2}. P_{MITOo2} is mitochondrial P_{O_2}. It should be noted that the substitution of P_{CAPo2} for effluent venous P_{O_2} (which closely approximates mean end capillary P_{O_2} [27]) eliminates uncertainties about the calculation of mean capillary P_{O_2} but does not qualitatively affect the conclusions of this study (Fig. 5 *B*).

Based on direct measurements of intracellular P_{O_2} (28) and mathematical modeling (29) in maximally exercising muscle, previous analyses of diffusivity, not knowing P_{MITOo2}, have limited their calculations to $\dot{V}O_{2max}$ where it was assumed cellular P_{O_2} was very low (1–3 mmHg range) and so could be neglected (4, 6, 30, 31). The present study has demonstrated that the assumption of a low intracellular P_{O_2} at $\dot{V}O_{2max}$, relied upon in these initial investigations, was valid and in fact is the case even at submaximal exercise intensities eliciting only 50% of $\dot{V}O_{2max}$ (Fig. 4), at least in this particular form of exercise.

Figure 5 *A* illustrates the progressive increase in diffusional conductance in both hypoxia and normoxia from submaximal to maximal WRs. As described above, until this unique measurement of both intracellular and intravascular P_{O_2}, it was considered invalid to perform this analysis at any point other than $\dot{V}O_{2max}$ because of uncertainty about intracellular P_{O_2}. At these submaximal levels diffusional conductance was greater in hypoxia, but as WR_{MAX} was approached both calculated mean capillary and femoral venous P_{O_2} in hypoxia and normoxia exhibited proportionality to the achieved leg $\dot{V}O_{2max}$. (Fig. 5 *B*, Table I). This single level of diffusional conductance at WR_{MAX} is consistent with other studies (8, 30, 31) and the theory that diffusion limitation may play a role in determining $\dot{V}O_{2max}$ in exercising muscle (4).

The effective diffusivity at submaximal WRs in hypoxia was markedly elevated in comparison to normoxic values. At $\approx$ 65% of $\dot{V}O_{2max}$ the diffusional conductance in hypoxia was already 85% of the maximum recorded value, whereas in normoxia at a comparable $\dot{V}O_2$ conductance was only 59% of the maximum value (Table I, Fig. 5 *A*). This difference may be the result of the increased concentration of available O_2 carrier within the muscle tissue (deoxy-Mb) (32) (Fig. 7).

The role of $\dot{V}O_2/\dot{Q}$ heterogeneity and the spatial averaging of the deoxy-Mb signal. When considering the importance of O_2 diffusivity in determining the large O_2 gradient from blood to myoglobin-associated P_{O_2} (Fig. 4, Table I), it is important to address the role of $\dot{V}O_2/\dot{Q}$ heterogeneity as a phenomenon which can produce similar results (33). To objectively quantify the influence of $\dot{V}O_2/\dot{Q}$ heterogeneity under these experimental conditions, we considered the possible scenario in which all venous P_{O_2} was the result of only heterogeneity, with no diffusion limitation. In this situation, when there is zero heterogeneity, $\dot{V}O_2$ is equal to the product of $\dot{Q}$ and CaO_2 (O_2 supply) and venous P_{O_2} must be zero. Thus, with this conceptual starting point and the data collected during maximal normoxic exercise, we calculated the necessary change in $\dot{V}O_2/\dot{Q}$ distribution (as estimated using log SD_Q, the second moment of the perfusion distribution on a log scale) that would result in a venous P_{O_2} of 22.1 mmHg, (as measured in the femoral vein at maximal exercise, Table I). The log SD_Q which satisfied this measured venous P_{O_2} was 0.55. To put this figure in perspective, we used the same SD_Q calculations to produce an estimate of muscle mass/$\dot{Q}$ distribution in a maximally exercising in situ canine gastrocnemius preparation (34) (modified to reduce surgical procedures and tissue traumatization [35]), injected with colored microspheres, and sectioned into 12 pieces after exercise. The log SD_Q for this preparation was only 0.13. Hence, we had to theoretically impose a fourfold greater maldistribution of $\dot{Q}$ than recorded in the surgically prepared canine muscle preparation to account for the venous P_{O_2} in our subjects through heterogeneity alone. Consequently, although this analysis can not quantifiably determine or discount the role of heterogeneity in producing the measured O_2 gradients, it does suggest that it is unlikely that these healthy subjects would demonstrate a $\dot{V}O_2/\dot{Q}$ heterogeneity that is significantly greater than that observed in the surgically prepared, electrically stimulated, in situ canine gastrocnemius preparation.

The deoxy-Mb spectra collected represent the spatial average signal across the region beneath the surface coil and therefore cannot provide insight into the distribution of deoxy-myoglobin at the intracellular level. Research at the cellular level has suggested that O_2 gradients within the cell are shallow and no anoxic loci have been found during exercise (36). Any heterogeneity in myoglobin saturation is minimized by the arrangement of the microvascular units (37) and the facilitated diffusion and redistribution of O_2 performed by myoglobin itself (38).

Rapid myoglobin desaturation at submaximal exercise. The maximum deoxy-myoglobin signal was apparent even at 50% of $\dot{V}O_{2max}$ (Fig. 7) and this desaturation occurred very rapidly (within a 20-s time frame, Fig. 6 *A*). The latter observation was highlighted during a single data collection period in the magnet by the rapid disappearance of the deoxy-myoglobin signal (resaturation) when exercise was ceased for < 45 s to adjust a subject's shin brace. Upon recommencement of the knee-extensor exercise the deoxy-myoglobin signal was again apparent and had returned to its previous value within the time resolution of the MRS system (20 s). This emphasizes that it would be inappropriate to attempt to measure intracellular P_{O_2} via myoglobin saturation with MRS by placing a subject in a magnet immediately after exercise. Additionally, this rapid myoglobin desaturation to 50–60% is indicative of the immediate use of at least half of the myoglobin O_2 stores. Thus, the speed and magnitude of this response may have several functions. First, the immediate availability of 50% of the stored myoglobin-associated O_2 may be an important O_2 source for the increased oxidative metabolism at the start of exercise. Second, this myoglobin desaturation reduces the carrier-depleted region, maximizing the P_{O_2} gradient from blood to cell. Consequently, the passive transport system responsible for O_2 influx into the muscle cell is facilitated by this rapid desaturation, even during light exercise. The greater deoxy-myoglobin signal in hypoxia (Fig. 7) and the concurrent elevation in the O_2 diffu-

sional conductance in hypoxia throughout submaximal exercise (Fig. 5), substantiates these observations.

Unaltered deoxy-myoglobin associated P_{O_2} from submaximal to maximal exercise. Both intuition and theoretical modeling (39) suggest it is reasonable to expect intracellular P_{O_2} to fall as the intensity of exercise increases to enhance the O_2 flux into the muscle cell (Eq. 2). The present data do not illustrate a fall in myoglobin saturation and thus intracellular P_{O_2} beyond that achieved in moderate exercise. However, as Eq. 2 illustrates, DO_2 also regulates O_2 flux. A major determinant of DO_2 is the effective surface area available for diffusion (40). If DO_2 increases in response to capillary recruitment and increased dynamic hematocrit (41–43), myoglobin-associated P_{O_2} need not change with increasing exercise intensity. In fact, consistent with this analysis, the calculated DO_2 for the present data did increase with each increased WR (Fig. 6). Thus, this study reveals that the O_2 conductance is recruited proportionally as $\dot{V}O_2$ increases (Fig. 5 *A*), but P_{MbO_2} remains constant after an initial fall during exercise eliciting submaximal $\dot{V}O_2$.

Muscle bioenergetics. The present MRS data represent the first continuous analyses of intramuscular bioenergetics in the rectus femoris during knee-extensor exercise. These data are similar to previous findings using other exercise modalities (17, 44). However, as recognized earlier, because the lowest intensity of knee-extensor exercise performed equated to $\approx$ 50% of $\dot{V}O_{2max}$, these data reveal a rapid change in muscle metabolism and pH during initial submaximal exercise. In fact, PCr fell from normal initial resting values to almost total depletion at WR_{MAX} and muscle pH fell to very low levels in both hypoxia and normoxia (Table II, Fig. 6 *B* and *D*). The concentration of Pi demonstrated a concomitant rise from resting levels (Table II, Fig. 6 *C*). These indicators of muscle metabolism, collected concurrently with the myoglobin spectra, are of significant importance as they illustrate that the proton MRS data were collected under conditions of high metabolic demand. Additionally, as these ^{31}P data are similar to previous measurements, made in this (45) and other human muscles with different exercise modalities (26), it is probable that the concurrent measurements of myoglobin saturation are not unique to this form of exercise and may be generalizable to other forms of dynamic exercise in humans.

Myoglobin P_{O_2} as a determinant of cellular respiration. This study has determined that myoglobin becomes significantly desaturated at submaximal exercise levels ($\approx$ 50% of $\dot{V}O_{2max}$) and remains at this level of desaturation even as leg $\dot{V}O_2$ is increased to maximum (Fig. 7). However, a secondary observation was that in hypoxia the degree of myoglobin desaturation was significantly greater than in normoxia and that this difference in O_2 saturation was still evident at leg $\dot{V}O_{2max}$ (Table I). It is not apparent from these data why, at normoxic WR_{MAX}, myoglobin-associated P_{O_2} did not fall to the level reached in hypoxia and why under both conditions desaturation was far less at WR_{MAX} than under conditions of cuff occlusion. In an effort to reconcile these questions, Fig. 8 illustrates that the present data support the hypothesis that leg $\dot{V}O_{2max}$ is dependent on myoglobin-associated P_{O_2} (Figs. 5 *B* and 8 *B*) and may represent an in vivo correlate (in myocytes) of the effect of O_2 tension on cellular respiration rate (in kidney cells) as previously described in vitro by Wilson et al. (46) (Fig. 8 *A*). The proportional relationship illustrated between leg $\dot{V}O_2$ and measured myoglobin-associated P_{O_2} and that this relationship, if continued, would pass through the origin (Fig. 8 *B*) are similar

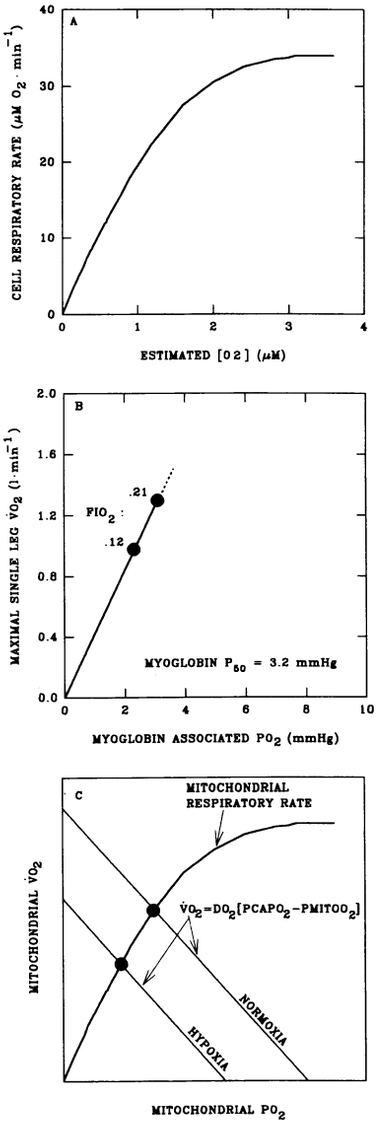

Figure 8. A comparison of the relationship between mitochondrial respiratory rate and O_2 availability in vitro made by Wilson et al. (46) (*A*) with the present in vivo measurements of the relationship between muscle $\dot{V}O_2$ and intracellular P_{O_2} (*B*). *C* theoretically combines the previous relationship described by Wilson et al. with the present observations to illustrate how the myoglobin-associated P_{O_2} data may fit with the O_2 supply dependance of $\dot{V}O_{2max}$ in intact normal humans.

to the findings of Wilson et al. (46) who found a hyperbolic relationship between O_2 tension and cellular respiratory rate in kidney cells (Fig. 8 *A*). It is speculated that these findings may represent initial data in the development of a hyperbolic relationship between in vivo muscle $\dot{V}O_2$ and intracellular P_{O_2}, supporting the concept that maximal respiratory rate ($\dot{V}O_{2max}$) is limited by O_2 supply (Fig. 8 *B*). We hypothesize that our data may describe a similar relationship to those of Wilson et al. (46) by reconciling the hyperbolic expression of O_2 utilization in Fig. 8 *A* with the linear expression of O_2 transport in Eq. 2, as theoretically illustrated in Fig. 8 *C*. Thus, Eq. 2, when $\dot{V}O_2$ is plotted against P_{MITOo2}, is a straight line of similar slope (DO_2) in normoxia and hypoxia but with a lower intercept in hypoxia due to the lower P_{CAPo2} at $\dot{V}O_{2max}$ (Table I). The intersection of these lines with the intrinsic mitochondrial $\dot{V}O_2/P_{O_2}$ hyperbolic relationship shows how the present myoglobin-associated P_{O_2} data fit with O_2 supply dependence of $\dot{V}O_{2max}$ in intact normal humans. The conclusions are identical, but the data are essentially independent of those relating $\dot{V}O_{2max}$ to mean capillary P_{O_2} in Fig. 5 *B*.

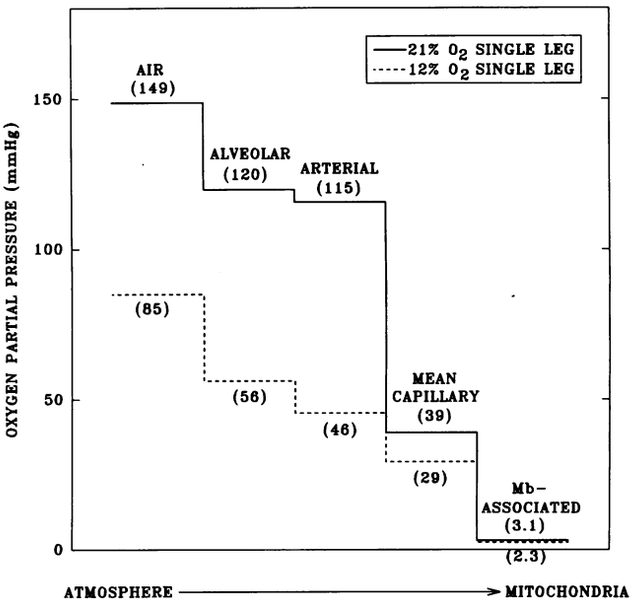

Figure 9. The complete oxygen cascade from the atmosphere to the muscle tissue during maximal knee-extensor exercise in both hypoxia and normoxia.

Oxygen cascade from air to tissues. Although theoretical figures similar in form to Fig. 9 are common, often used as teaching aids (47), the ability to construct Fig. 9 from actual data has potential diagnostic use. These in vivo data collected in normal humans illustrate the potential clinical use of combining techniques to further elucidate the underlying pathophysiology of disease states which affect this oxygen cascade by identifying where the compromise in O_2 transport occurs.

Summary. The combination of isolated human quadriceps exercise and MRS technology in this study allowed the unique analysis of O_2 gradients from the air to tissue in humans. These data provide evidence of a substantial O_2 gradient from blood to tissue, suggesting a resistance to the diffusion of O_2 between red cell and sarcolemma, and that this is present even during submaximal exercise. As WR is increased and O_2 demand is elevated, O_2 flux can be increased despite this diffusion limitation, presumably by increasing the area available for diffusion by increasing both blood flow and capillary recruitment. Diffusional conductance was consistently elevated in hypoxia, as was the level of deoxy-myoglobin. Thus, influenced heavily by the increased magnitude of myoglobin-facilitated O_2 flux in hypoxia, the reduction in intracellular resistance from sarcolemma to cell interior may account for the enhanced diffusional conductance at submaximal WRs. As maximal $\dot{V}O_2$ was approached in normoxia, diffusional conductance continued to rise and match the diffusional conductance in hypoxia at WR_{MAX}, despite no increase in myoglobin desaturation. This was probably made possible by the continued ability to perform work in normoxia and the resulting increase in blood flow that this dictates. The ability to measure tissue P_{O_2} in hypoxia and normoxia reveals that at muscle $\dot{V}O_{2max}$ tissue O_2 diffusional conductance is equal and mean capillary P_{O_2}, femoral venous P_{O_2}, myoglobin P_{O_2}, and maximal $\dot{V}O_2$ are each reduced proportionately in hypoxia supporting the concept that O_2 supply plays a role in determining $\dot{V}O_{2max}$.

Acknowledgments

The authors express their appreciation to the subjects who participated in this study. We also thank Drs. Bruno Grassi, David Poole, Douglas Knight, Kipp Erickson, Hideo Michimata, Britton Chance, Lizann Bolinger, Ravi Reddy, and Erick Insko for their invaluable assistance. Additionally, we are as usual indebted for the expert technical assistance of Harrieth Wagner, Nick Busan, Jeffrey Struthers, and Alan Bonner.

Dr. Richardson was directly funded by a fellowship from the American Lung Association of California during this research. This study was additionally supported by the Cigarette and Tobacco Surtax Fund of the State of California through the Tobacco Related Disease Research Program of the University of California grant RT 227 and also by National Heart, Lung, and Blood Institute grants HL-17731 and HL-44125.

References

1. Wang, Z., E. A. Noyszewski, and J. S. Leigh. 1990. In vivo MRS measurement of deoxymyoglobin in human forearms. *Magn. Reson. Med.* 14:562–567.

2. Thomas, A., and P. G. Morris. 1981. The effects of NMR exposure on living organisms. A microbial assay. *Br. J. Radiol.* 54:615–621.

3. Donald, K. W., P. N. Wormald, S. H. Taylor, and J. M. Bishop. 1957. Changes in the oxygen content of femoral venous blood and leg blood flow during leg exercise in relation to cardiac output response. *Clin. Sci. (Lond.).* 16:567–591.

4. Wagner, P. D. 1992. Gas exchange and peripheral diffusion limitation. *Med. Sci. Sports Exercise.* 24:54–58.

5. Andersen, P., R. P. Adams, G. Sjogaard, A. Thorbe, and B. Saltin. 1985. Dynamic knee extension as a model for study of isolated exercising muscle in humans. *J. Appl. Physiol.* 59:1647–1653.

6. Richardson, R. S., D. R. Knight, D. C. Poole, S. S. Kurdak, M. C. Hogan, B. Grassi, and P. D. Wagner. 1995. Determinants of maximal exercise VO_2 during single leg knee extensor exercise in man. *Am. J. Physiol.* 268:H1453–H1461.

7. Richardson, R. S., S. C. Johnson, and M. S. Walker. 1992. Heart rate VO_2 relationship changes following intense training. *Sports Med., Training, and Rehab.* 3:105–111.

8. Richardson, R. S., D. C. Poole, D. R. Knight, S. S. Kurdak, M. C. Hogan, B. Grassi, E. C. Johnson, K. Kendrick, B. K. Erickson, and P. D. Wagner. 1993. High muscle blood flow in man: is maximal O_2 extraction compromised? *J. Appl. Physiol.* 75:1911–1916.

9. Poole, D. C., G. A. Gaesser, M. C. Hogan, D. R. Knight, and P. D. Wagner. 1992. Pulmonary and leg VO_2 during submaximal exercise: implications for muscular efficiency. *J. Appl. Physiol.* 72:805–810.

10. Andersen, P., and B. Saltin. 1985. Maximal perfusion of skeletal muscle in man. *J. Physiol. (Camb.).* 366:233–249.

11. Bangsbo, J., P. D. Gollnick, T. E. Graham, C. Juel, B. Kiens, M. Mizuno, and B. Saltin. 1990. Anaerobic energy-production and O_2 deficit-debt relationship during exhaustive exercise in humans. *J. Physiol. (Camb.).* 422:539–559.

12. Knight, D. R., D. C. Poole, W. Schaffartzik, H. J. Guy, R. Prediletto, M. C. Hogan, and P. D. Wagner. 1992. Relationship between body and leg VO_2 during maximal cycle ergometry. *J. Appl. Physiol.* 73:1114–1121.

13. Rowell, L. B., B. Saltin, B. Kiens, and N. J. Christensen. 1986. Is peak quadriceps blood flow in humans even higher during exercise with hypoxemia? *Am. J. Physiol.* 251:H1038–H1044.

14. Schnall, M. D., V. H. Subramanian, J. S. Leigh, and B. Chance. 1985. A new double-tuned probe for concurrent ^1H and ^{31}P NMR. *J. Mag. Reson.* 65:122–129.

15. Bertinini, I., and C. Luchinat. 1986. NMR Paramagnetic Molecules in Biological Systems. The Benjamin-Cummings Publishing Co., Menlo Park, CA.

16. Harris, R., E. Hultman, and L. O. Nordesjo. 1974. Glycogen, glycolytic intermediates, and high-energy phosphates determined in biopsy samples of musculus quadriceps femoris of man at rest. Methods and variance values. *Scand. J. Clin. Lab. Invest.* 33:109–120.

17. Sapega, A. A., D. P. Sokolow, T. J. Graham, and B. Chance. 1987. Phosphorus nuclear magnetic resonance: a non-invasive technique for the study of muscle bioenergetics during exercise. *Med. Sci. Sports Exercise* 19:410–420.

18. Taylor, D. J., P. Styles, P. M. Mathews, D. A. Arnold, D. G. Gadian, P. Bore, and G. K. Radda. 1986. Energetics of human muscle: exercise-induced ATP depletion. *Magn. Reson. Med.* 3:44–54.

19. Kreutzer, U., Y. Chung, D. Butler, and T. Jue. 1993. H-NMR characterization of the human myocardium myoglobin and erythrocyte hemoglobin signals. *Biochim. Biophys. Acta.* 1161:33–37.

20. Wang, D. J., S. Nioka, Z. Wang, J. S. Leigh, and B. Chance. 1993. NMR visibility studies of N-sigma proton of proximal histidine in deoxyhemoglobin in lysed red blood cells. *Magn. Reson. Med.* 30:759–763.

21. Blei, M. L., K. E. Conley, and M. J. Kushmerick. 1993. Separate measures of ATP utilization and recovery in human skeletal muscle. *J. Physiol. (Camb.).* 465:203–222.

22. Rossi-Fanelli, A., and E. Antonini. 1958. Studies of the oxygen and carbon monoxide equilibria of human myoglobin. *Arch. Biochem. Biophys.* 77:478–492.

23. Saltin, B., and L. Hermansen. 1966. Esophageal, rectal and muscle temperature during exercise. *J. Appl. Physiol.* 21:1757–1762.

24. Jones, P. R. M., and J. Pearson. 1969. Anthropometric determination of leg fat and muscle plus bone volumes in young male and female adults. *J. Physiol. (Camb.).* 294:63P–66P.

25. Richardson, R. S., D. C. Poole, D. R. Knight, and P. D. Wagner. 1994. Red blood cell transit time in man: theoretical effects of capillary density. *In* Advances in Experimental Medicine and Biology. D. C. Hogan, O. Mathieu-Costello, D. C. Poole, and P. D. Wagner, editors. Plenum Publishing Corp., New York. 521–532

26. Systrom, D. M., D. J. Kanarek, S. J. Kohler, and H. Kazemi. 1990. ^{31}P nuclear magnetic resonance spectroscopy study of the anaerobic threshold in humans. *J. Appl. Physiol.* 68:2060–2066.

27. Honig, C. R., T. E. Gayeski, A. Clark, and P. A. A. Clark. 1991. Arteriovenous oxygen shunt is negligible in resting and working gracilis muscles. *Am. J. Physiol.* 261:H2031–2043.

28. Gayeski, T. E. J., and C. R. Honig. 1988. Intracellular PO_2 in long axis of individual fibers in working dog gracilis muscle. *Am. J. Physiol.* 254 (*Heart Circ. Physiol.)* 23:H1179–H1186.

29. Groebe, K., and G. Thews. 1988. Theoretical analysis of oxygen supply to contracted skeletal muscle. *Adv. Exp. Med. Biol.* 222:25–35.

30. Hogan, M. C., J. Roca, J. B. West, and P. D. Wagner. 1989. Dissociation of maximal O_2 uptake from O_2 delivery in canine gastrocnemius in situ. *J. Appl. Physiol.* 66:1219–1226.

31. Knight, D. R., W. Schaffartzik, D. C. Poole, M. C. Hogan, D. E. Bebout, and P. D. Wagner. 1993. Hyperoxia increases leg maximal oxygen uptake. *J. Appl. Physiol.* 75:2586–2594.

32. Honig, C. R., and T. E. J. Gayeski. 1993. Resistance to O_2 diffusion in anemic red muscle: role of flux density and cell PO2. *Am. J. Physiol.* 265:H868–H875.

33. Piiper, J., and P. Haab. 1991. Oxygen supply and uptake in tissue models with unequal distribution of blood flow and shunt. *Respir. Physiol.* 84:261–271.

34. Hogan, M. C., R. S. Richardson, and S. S. Kurdak. 1994. Initial fall in skeletal muscle force development during ischemia is related to oxygen availability. *J. Appl. Physiol.* 77:2380–2384.

35. Piiper, J. 1990. Unequal distribution of blood flow in exercising muscle of dog. *Respir. Physiol.* 80:129–136.

36. Gayeski, T. E. J., and C. R. Honig. 1986. O_2 gradients from sarcolemma to cell interior in a red muscle at maximal VO2. *Am. J. Physiol.* 251:789–799.

37. Lunde, N., D. N. Damon, and B. R. Duling. 1987. Capillary grouping in hamster tibialis anterior muscle: flow patterns and physiological significance. *Int. J. Microcirc. Clin. Exp.* 5:359–372.

38. Wittenburg, B. A., and J. B. Wittenberg. 1989. Transport of oxygen in muscle. *Annu. Rev. Physiol.* 51:857–878.

39. Severinghaus, J. W. 1994. Exercise O_2 transport model assuming zero cytochrome PO_2 at VO_2max. *J. Appl. Physiol.* 77:671–678.

40. Federspiel, W. J., and A. S. Popel. 1986. A theoretical analysis of the effect of the particulate nature of blood on oxygen release in capillaries. *Microvasc. Res.* 32:164–189.

41. Lindbom, L., R. F. Tuma, and K. E. Arfors. 1980. Influence of oxygen on perfused capillary density and capillary red cell velocity in rabbit skeletal muscle. *Microvasc. Res.* 19:197–208.

42. Honig, C. R., C. L. Odoroff, and J. L. Frieson. 1982. Active and passive control in red muscle at rest and in exercise. *Am. J. Physiol.* 243:H196–H206.

43. Gorzynski, R. J., and B. R. Duling. 1978. Role of oxygen in functional vasodilation in hamster striated muscle. *Am. J. Physiol.* 235:H505–H515.

44. Hultman, E., J. Bergstrom, and N. Anderson. 1967. Breakdown and resynthesis of phosphoylctreatine and adenosine triphosphate in connection with muscular work in man. *Scand. J. Clin. Lab. Invest.* 19(1):55–66.

45. Bangsbo, J., T. Graham, L. Johansen, and B. Saltin. 1994. Muscle lactate metabolism in recovery from intense exhaustive exercise: impact of light exercise. *J. Appl. Physiol.* 77:1890–1895.

46. Wilson, D. F., M. Erecinska, C. Drown, and I. A. Silver. 1977. Effect of oxygen tension on cellular energetics. *Am. J. Physiol.* 233:C135–C140.

47. West, J. B. 1984. Respiratory Physiology-The Essentials. 3rd edition. Williams and Wilkins, Baltimore. 55.